Applied Microscopy
Korean Society of Microscopy

pISSN 2287-5123 · eISSN 2287-4445
https://doi.org/10.9729/AM.2018.48.2.43

Review Article

Phase Transformation of Two-Dimensional Transition Metal Dichalcogenides

Jaemin Kim, Zonghoon Lee*

School of Materials Science and Engineering, Ulsan National Institute of Science and Technology, Ulsan 44919, Korea

*Correspondence to:
Lee Z,
http://orcid.org/0000-0003-3246-4072
Tel: +82-52-217-2327
Fax: +82-52-217-2309
E-mail: zhlee@unist.ac.kr

Received June 7, 2018
Revised June 21, 2018
Accepted June 21, 2018

Transition metal dichalcogenide (TMD) materials have distinctive structures in comparison with other two-dimensional materials. TMD materials' structure is held together by van der Waals and covalent intralayer interactions; consequently, TMDs exhibit multiple phases and properties depending on their structure. This article reviews some of the research currently being undertaken to control TMD phases to utilize their different properties. This review introduces some trials for changing the phase of TMDs.

Key Words: Two-dimensional materials, Phase transformation, Transition metal dichalcogenide

INTRODUCTION

Transition metal dichalcogenides (TMDs) exhibit layered structures which have three atomic interlayered structure. In TMDs, one transition-metal (M) layer is sandwiched between two chalcogen (X) layers, with MX_2 stoichiometry. Because of this three-atom layer structure, multiple phases can exist within the crystal structure. TMDs can have trigonal prismatic (2H) and octahedral (1T) phase structures (Fig. 1). In the 2H phase, a single (S) layer of atoms are vertically aligned; thus, the stacking state of this phase shows ABA, where A is the chalcogen layer and B is the transition-metal layer. In the case of the 1T phase, one of the S layers is shifted relative to the other. Due to this state, it exhibits ABC stacking sequences. These differences are influenced by the d-orbital filling of the transition-metal atom. In the 2H phase, the d orbital splits into d_{z^2},($d_{x^2-y^2}$ d_{xy}), and (d_{yz} d_{xz}) of three degenerated states. However, in the case of the 1T phase, the d orbital splits into (d_{xy} d_{yz} d_{zx}) and ($d_{x^2-y^2}$ d_{z^2}) orbitals. Because chalcogens' p orbitals have lower energy than the Fermi level, only the d-orbital filling determines the structure of the TMDs. Filled orbitals result in semiconductor properties and partially filled orbitals result in metallic properties. Group 4 and 6 TMDs usually exhibit 2H phases, group 5 can have both 2H and 1T phase, group 7 exhibits distorted 1T phases, and group 10 exhibits 1T structures (Chhowalla et al., 2013; Duerloo & Reed, 2016; Duerloo et al., 2014; Eda et al., 2011, 2012; Voiry et al., 2015).

A single-layer TMD can have two types of 2H- and 1T-phase states in a single layer. In a multilayer state, depending on the stacking sequence, a TMD can also exhibit 3R symmetry. 2H symmetry displays stacking sequences like ABA BAB; however, in the 3R case, the stacking sequence will be ABA CAC BCB. However, no other symmetry exists in the 1T state.

INTERCALATION

The mostly wide used method for phase transition of TMDs is lithium intercalation. If alkali metals are intercalated into the layered TMDs, the alkali metals become the reducing agent of the transition metal by transferring electrons to lower unoccupied molecular orbitals of the TMDs. This causes structural changes in the host metal atom. When phase transition by lithium intercalation occurs, transmission electron microscope (TEM) and X-ray photoelectron spectroscopy analysis indicate the formation of superlattice of Mo atoms (Fig. 2). In the case of MoS_2 exfoliation by lithium intercalation, distortion arose in (2a×a) zigzag chains such as those in WTe_2.

This intercalation reaction occurs with lithium reactants, such as n-butyllithium. TMDs react with the lithium reactant until

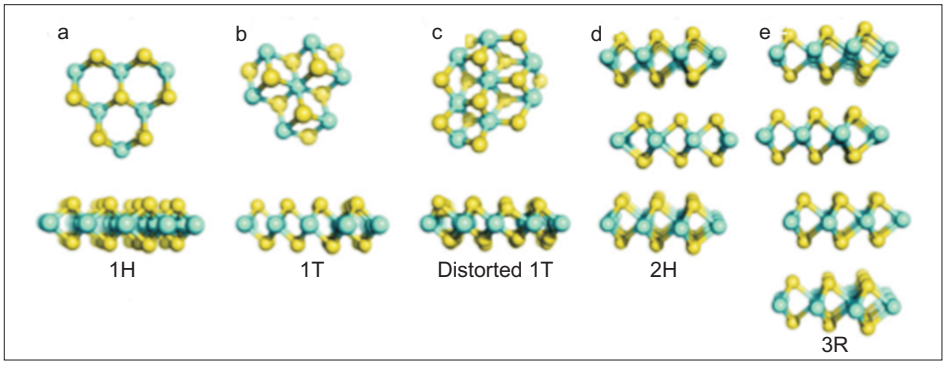

Fig. 1. Types of transition metal dichalcogenide structures. Chalcogen atoms are shown in yellow, and transition metal atoms are shown in blue. (A) 1H phase; (B) 1T phase; (C) distorted 1T or 1T′ phase; (D) 2H phase; (E) 3R phase. Reprinted from the article of Voiry et al. (2015) (*Chem Soc Rev* 44, 2702-2712) with Chemical Society Reviews' permission.

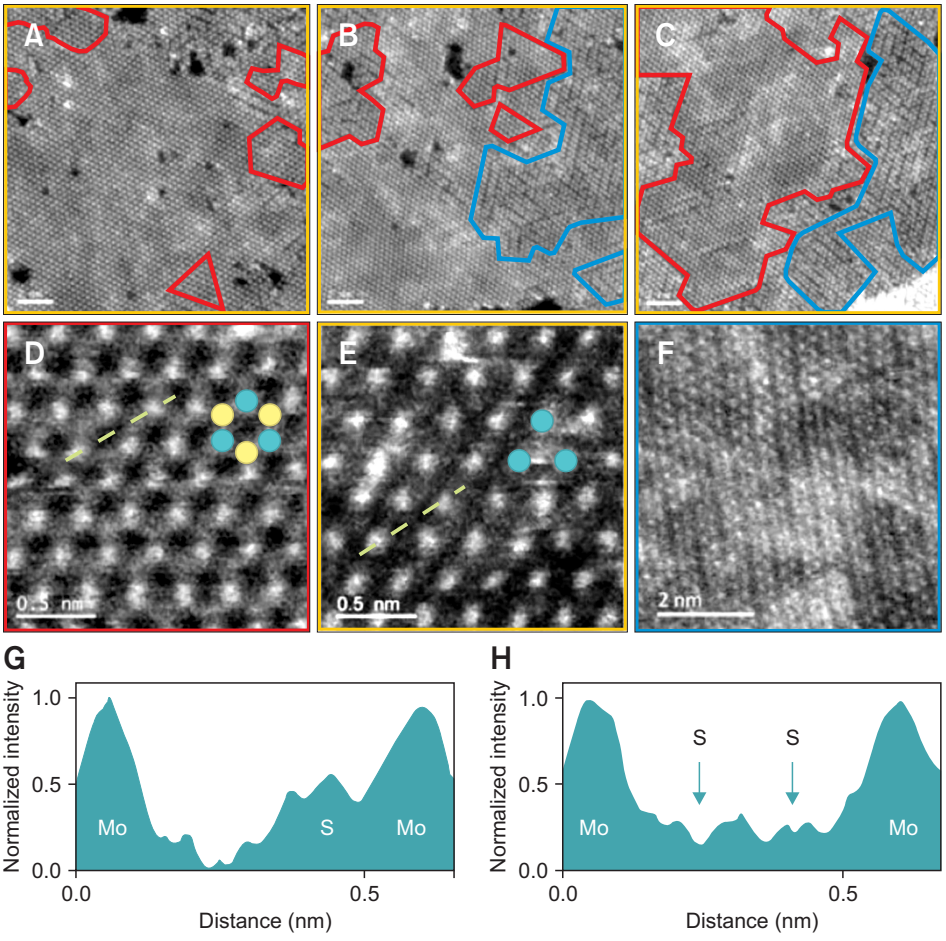

Fig. 2. Scanning transmission electron microscope (STEM) images of various regions of chemically exfoliated monolayer MoS_2. The 2H phase is in red, the 1T phase is in yellow, and the distorted 1T phase is in blue. (A-C) 2H structural domains are observed in a region where the 1T phase is dominant. High-resolution STEM images of 2H (D), 1T (E), and distorted 1T (F) phases. In images Fig. 2D and E, the blue dots indicate Mo and the yellow dots indicate S atoms. Intensity profiles along the lines indicated in images Fig. 2D and E are shown in images Fig. 2G and H, respectively. Scale bars=2 nm (A-C), 0.5 nm (D and E), 2 nm (F). Reprinted from the article of Eda et al. (2012) (*ACS Nano* 6, 7311-7317) with American Chemical Society's permission.

lithium sufficiently intercalated into materials. The reaction time is different for each specimen. MoS_2 exhibits low reactivity in the intercalation reaction, unlike TiS_2, and requires a long time, one or two days, for an appreciable degree of intercalation. Lithium intercalated TMDs are washed with hexane to remove organic byproducts and reactants (Benavente, 2002).

Using microwave assisted reactions, reaction times can be reduced, and good quality results obtained for MoS_2. This process results in the enhanced diffusion of lithium into the matrix. Other methods to accelerate MoS_2 intercalation also exist. According to Fan et al. (2015), lithium intercalation can be accelerated by sonication, resulting in the time required to decrease in the scale of minutes. Sonication helps overcome the activation barrier for intercalation by facilitating the transient expansion and exfoliation of layered materials in a liquid suspension (Benavente & González, 1997).

The other way for intercalation of alkali metal to TMDs is electrochemical method: Zeng et al. (2011) used bulk TMD

as a cathode and Li metal as an anode to intercalate Li ions between TMD layers. For the MoS_2 case, they reported a transition to the 1T phase and reported that wherever over insertion occurred, MoS_2 decomposition also occurred. This method also requires a long reaction time to obtain a significant amount of product. However, it has the advantage of easily providing information about thermodynamics and kinetics, and intercalation can be quantitatively followed using coulometry (Zeng et al., 2011).

These TMD-intercalation processes are reversible reactions. For group 6 TMDs, the 2H phase is more stable than the 1T phase in the normal state. If excessive charge is added, the 2H phase becomes unstable and a transition to the 1T phase occurs; however, the excessive charge is removed when the lithium ion removed from the TMDs. After that, 1T phase TMDs is returned to the most stable 2H phase. However, the driving force caused by stability is not enough to jump the energy barrier for phase transition to the 2H phase: its lattice structure distorts to relieve the unstable structure (Ambrosi et al., 2015; Kan et al., 2014; Kappera et al., 2014).

PHASE TRANSITION WITHOUT INTERCALATION

Fan et al. (2015) found that an IR laser induced the 2H phase restoration process. They spread chemically exfoliated MoS_2 onto a DVD disk and irradiated it using an IR laser onto the optical drive of a DVD. Using this method, phase restoration was completed in just one write cycle. Phase restoration was indicated by the disk changing color from black to light gray, and was verified by Raman spectroscopy. After phase restoration, the characteristic peaks of the 1T phase superlattice disappeared.

Other methods for phase transition of TMDs have been researched. Lin et al. (2014) stimulated a TMD layer with an electron beam, and using scanning transmission electron microscope (STEM) for the electron-beam projection, observed changes in the TMD layer in situ (Fig. 3). They used a 2H-phase MoS_2 specimen doped with Re at about 0.6 at%. The specimen was heated in situ to between 400°C and 700°C to promote phase transition. As a result, the 2H to 1T phase transition occurred accompanied with new phase boundaries. This process initially formed a precursor phase, the α-phase, which is an intermediate state that forms a stable structure under electron-beam irradiation. This phase has a strong tendency to nucleate Re dopants. Because of the effect of Mo–Mo constriction on this phase formation, S lattice out-of-plane displacement occurs, which can be propagated through the zigzag direction. When two α-phases meet via propagation, the 1T phase and phase boundary, β and γ, are generated. For

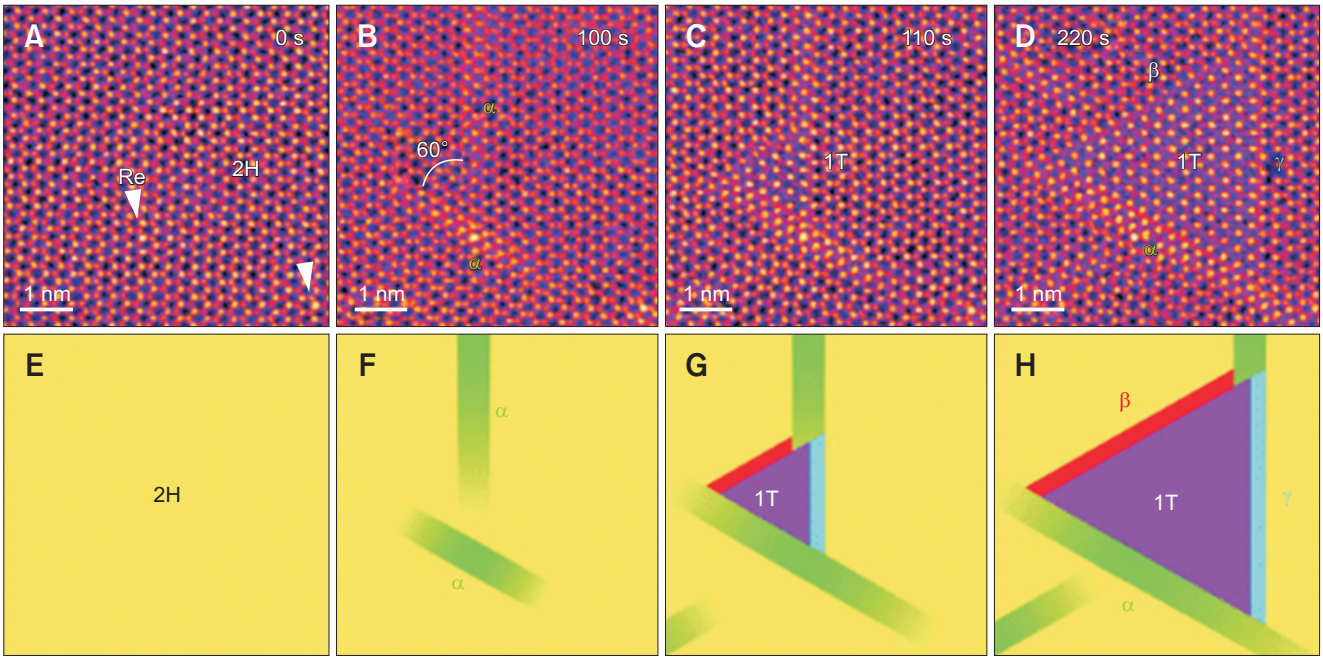

Fig. 3. Phase transition of MoS_2 at 600°C. (A) The Re-doped single-layer MoS_2 exhibits the initial 2H phase of a hexagonal lattice structure. (B) At *t*=100 s, two intermediate phases (denoted α) form with an angle of 60°. (C) At *t*=110 s, a triangular 1T phase appears in the corner between the two α-phases. The 1T phase exhibits a noticeable contrast because of the S atoms in the HC sites. (D) At *t*=220 s, the transformed 1T-phase area is enlarged. Three different boundaries (α, β, and γ) are found on the three edges between the 1T and 2H phases. (E-H) Simple schematic illustrations of the 2H→1T phase transition corresponding to the annular dark field images in Fig. A-D, respectively. (A-D) Scale bars=1 nm. Reprinted from the article of Lin et al. (2014) (*Nat Nanotechnol* 9, 391-396) with Nature Nanotechnology's permission.

this method, phase transition is involved via lattice gliding, and this phase transition occurs only in the area scanned by the electron beam (Lin et al., 2014).

Cho et al. (2015) investigated the phase patterning of $MoTe_2$ using a laser. When a high-energy laser was irradiated onto a $MoTe_2$ layer, the 2H phase distorted to the 1T phase (a WTe_2 like structure), and the phase transition was derived. They used Raman spectroscopy to define the phase transition. However, this method cannot avoid the thinning of the $MoTe_2$ layer due to laser irradiation. The Raman spectroscopy results revealed any contaminants such as oxides, and clearly showed heterophase homojunction structures. The reverse phase transition from 1T to 2H was not observed. The laser energy used in this method can be converted into temperatures of about 400°C. This temperature is less than the reported temperature for $MoTe_2$ phase transition (880°C). Because the reaction occurred at a lower temperature than the Te sublimation temperature (~400°C), the 2H phase region was reserved without Te vacancies (Cho et al., 2015).

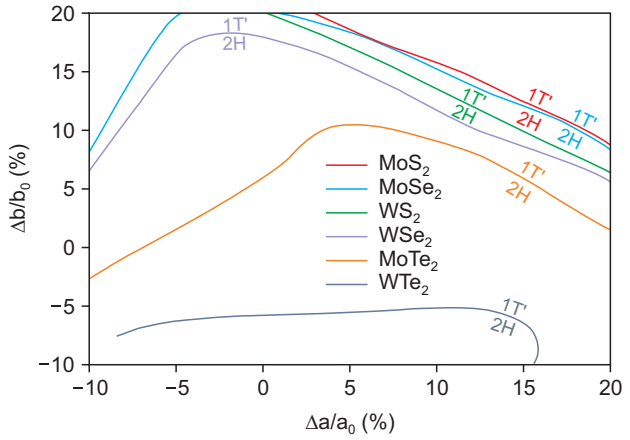

Fig. 4. 2H and distorted 1T energy surface intersection contours in a rectangular lattice constant ('a' and 'b'). The phases labeled on each side of contours are the lower energy phases. Reprinted from the article of Duerloo et al. (2014) (*Nat Commun* 5, 4214) with Nature Communications' permission.

Another method used for phase patterning uses Ar plasma. Zhu et al. (2017) experimented with this method and found that for 40 seconds treatment by Ar plasma, MoS_2 undergoes 2H to 1T phase transition. The principle of this method is similar to laser phase patterning, which creates chalcogen atom vacancies. The area hitting by plasma cannot be controlled by the delivery instrument; hence, undesired regions should be protected from the Ar plasma. They noted that if the treatment duration increased, increasing S defects eliminated the 1T phase (Zhu et al., 2017).

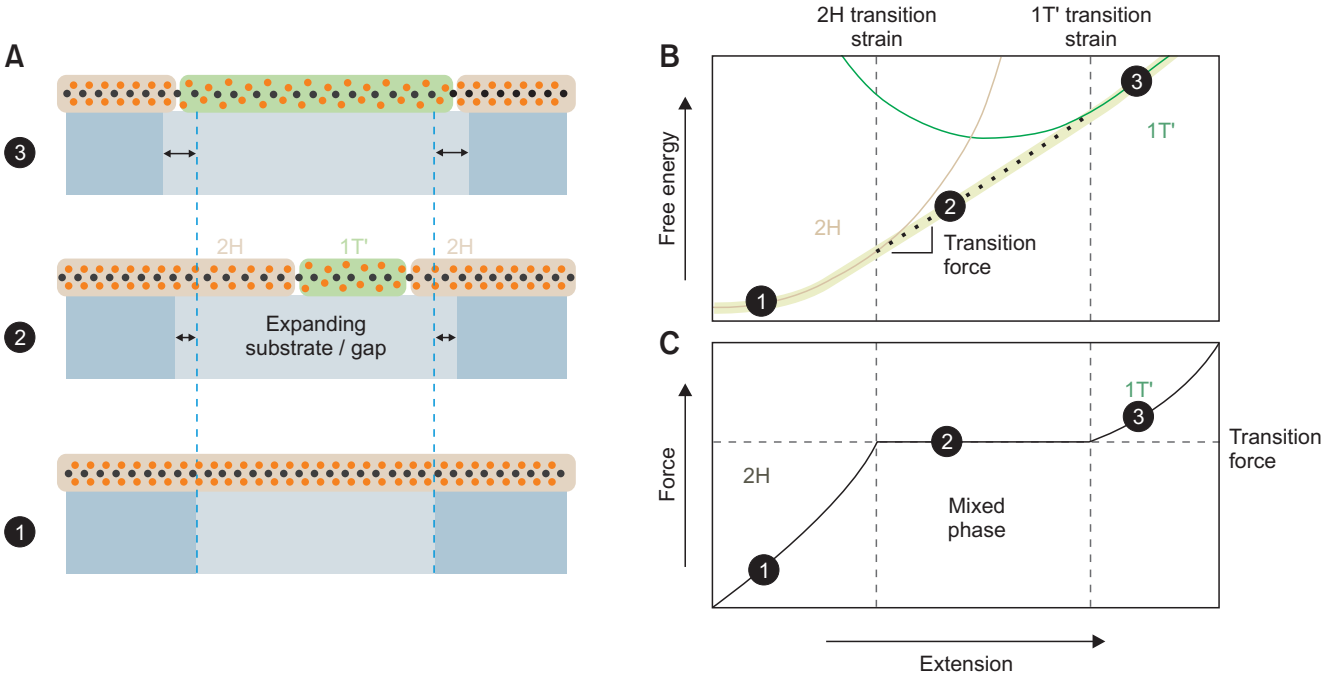

Fig. 5. Phase coexistence under applied tension. A tensile mechanical deformation expands transition metal dichalcogenide (TMD) monolayer. (A) Phase transitions of TMDs with uniaxial tensile stress. The low-friction substrate region (middle) undergoes phase transition. Change in free energy (B) and force (C) caused by uniaxial tensile stress. In step 1, the TMD exhibits elastic deformation in a 2H phase. In step 2, the tangent line of the 2H phase and the distorted 1T phase energy surface become the lowest free-energy path. In this region, the 2H and distorted 1T phase coexist. In step 3, the distorted 1T phase becomes the lowest energy state and the distorted 1T phase region is extended. Reprinted from the article of Duerloo et al. (2014) (*Nat Commun* 5, 4214) with Nature Communications' permission.

Those two methods are similar because they both create irreversible chalcogen vacancies, and these vacancies become the driving force for the phase transition from 2H to 1T. The reactions occur only in the area where the laser and/or plasma hit; thus, both techniques can be used for selective phase patterning or creating in-plane heterophase structures. However, these methods are destructive and cannot reverse the change from the 2H to 1T phase state.

STRAIN INDUCED PHASE TRANSITION

Strain can influence the TMD phase. Duerloo et al. (2014) demonstrated how tensile or compressive stress affects the phase transition of group 6 TMDs using density funtional calculation (DFT) calculations, and they derived the energy of the surface intersection between the 2H and 1T phases. Their results demonstrated that it is possible to transform a TMD phase from 2H to a distorted 1T (1T′) phase using reversible biaxial strain, which can also create heterophases from 100% 2H or distorted 1T phases, and this mixed phase is thermodynamically stable (Fig. 4). From their calculations, they found that only WTe_2 have a negative energy contour for group 6 TMDs, and this material exhibited a distorted 1T phase structure (Fig. 5). Following this contour, it might be inferred that compressional strain can form a 2H phase WTe_2 (Duerloo et al., 2014).

PHASE BOUNDARY

Lin et al. (2014) reported that some phase boundaries exist in heterophase TMDs; high-resolution TEM revealed that these phase boundaries are atomically sharp and have no visible defects. Phase boundaries exist as four types: α, β, β′, and γ (Fig. 6). The α-boundary comprises four-membered rings, three of which are chalcogen atoms and one is a metal atom. This phase is formed by the M–M distance compression in the zigzag chain. During the progress of the phase transformation, this phase returns to the original 2H phase. Because of this reversible process, the phase transition between 2H to α has no massive atomic loss. In the β-boundary, two aligned metal atoms are connected with two S atoms in a four-membered ring. This phase can also be found in 2H/2H′ twin boundaries. For the 2H to 1T phase transition, it has been shown that both metal and chalcogen planes glide during the phase transition process. The β′-boundary has the same structure as the β-boundary, but it is rotated by 30° either clockwise or counterclockwise. The γ-boundary comprises two separated four-membered rings, and these S atoms are in a zigzag chain containing α-phase-like rings rotated 60° (Hu et al., 2015; Lin et al., 2014).

Most of the methods for phase transition from 2H to 1T or distorted 1T are activated only at zigzag chains. Hu et al. (2015) determined this using DFT calculations for MoS_2 and WS_2. They derived that if the boundary phase (α, β, and γ) formed along an armchair edge, the 1T phase cannot be maintained during the relaxation period and transition from the 1T phase to the 2H phase. However, in the zigzag-chain case, the 1T phase is distorted and does not return to the 2H phase. This can be explained by an activation barrier difference between the phase transformation and the relaxation of the zigzag-chain distortion. Because the former is smaller than the latter, relaxation phase boundaries cannot be formed in the zigzag

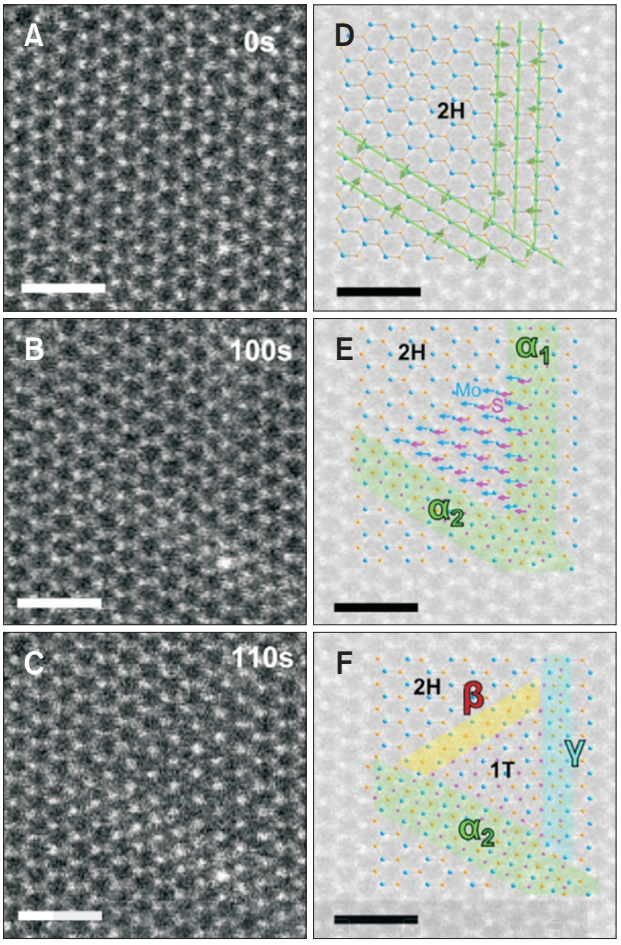

Fig. 6. (A-C) Sequential annular dark field (ADF) images clipped from Fig. 2A-C. (D-F) Transparent ADF images with the structural model overlaid. (A-F) Scale bars=1 nm. (D) Two nonparallel α-phases start forming in single-layer 2H-MoS_2 by constriction of three Mo zigzag chains. (E) A triangular shaped area of Mo+S (or S′) atoms glide a distance equivalent to the lattice constant in the direction indicated by the blue and pink arrows. (F) A triangular shaped area of 1T phase is formed after atomic-plane gliding. The α-phase (three Mo zigzag chains) behaves as a reservoir by emitting atoms that can be emit one Mo zigzag chain. The α-phase on the right-hand side (α1) is transformed to the γ-boundary (two Mo zigzag chains). The α2 accepted one zigzag chain of Mo atoms and reconstructed to a wider α-phase containing four Mo zigzag chains. Reprinted from the article of Lin et al. (2014) (*Nat Nanotechnol* 9, 391-396) with Nature Nanotechnology's permission.

direction (Hu et al., 2015).

CONCLUSIONS

Because TMDs exhibit multiple phases and their properties differ by phase, research has been focused on how to effect these phase changes. The intercalation method is the most widely used phase transition method and results in transitions between semiconducting and metallic properties. This method uses a reversible reaction and includes exfoliation from bulk to sheet TMDs. Chemical intercalation is mainly performed using an organolithium reagent as the reactant. However, the time required for the reaction differs by the type of TMD: materials like MoS_2 require about a day; therefore, many trials have attempted to accelerate the intercalation process using external stimulation or different techniques for intercalation. For selective phase transition, electron beams, lasers, and plasmas have been used successfully. The coexistence of semiconducting and metallic phase by phase engineering has been researched for use in electric devices such as transistors. Some of these are irreversible processes. Metallic phases formed by irreversible methods are unaltered by environmental changes, and this property is important for device reliability.

CONFLICT OF INTEREST

No potential conflict of interest relevant to this article was reported.

ACKNOWLEDGMENTS

This work was supported by the National Research Foundation of Korea (NRF) grant funded by the Korea government (MSIT) (no. 2018R1A2A2A05019598).

REFERENCES

Ambrosi A, Sofer Z, and Pumera M (2015) 2H --> 1T phase transition and hydrogen evolution activity of MoS2, MoSe2, WS2 and WSe2 strongly depends on the MX2 composition. *Chem. Commun. (Camb)* **51**, 8450-8453.

Benavente E (2002) Intercalation chemistry of molybdenum disulfide. *Coord. Chem. Rev.* **224**, 87-109.

Benavente E and González G (1997) Microwave activated lithium intercalation in transition metal sulfides. *Mater. Res. Bull.* **32**, 709-717.

Chhowalla M, Shin H S, Eda G, Li L J, Loh K P, and Zhang H (2013) The chemistry of two-dimensional layered transition metal dichalcogenide nanosheets. *Nat. Chem.* **5**, 263-275.

Cho S, Kim S, Kim J H, Zhao J, Seok J, Keum D H, Baik J, Choe D H, Chang K J, Suenaga K, Kim S W, Lee Y H, and Yang H (2015) Device technology. Phase patterning for ohmic homojunction contact in MoTe(2). *Science* **349**, 625-628.

Duerloo K A, Li Y, and Reed E J (2014) Structural phase transitions in two-dimensional Mo- and W-dichalcogenide monolayers. *Nat. Commun.* **5**, 4214.

Duerloo K A and Reed E J (2016) Structural phase transitions by design in monolayer alloys. *ACS Nano* **10**, 289-297.

Eda G, Fujita T, Yamaguchi H, Voiry D, Chen M, and Chhowalla M (2012) Coherent atomic and electronic heterostructures of single-layer MoS2. *ACS Nano* **6**, 7311-7317.

Eda G, Yamaguchi H, Voiry D, Fujita T, Chen M, and Chhowalla M (2011) Photoluminescence from chemically exfoliated MoS2. *Nano Lett.* **11**, 5111-5116.

Fan X, Xu P, Zhou D, Sun Y, Li Y C, Nguyen M A, Terrones M, and Mallouk T E (2015) Fast and efficient preparation of exfoliated 2H MoS2 nanosheets by sonication-assisted lithium intercalation and infrared laser-induced 1T to 2H phase reversion. *Nano Lett.* **15**, 5956-5960.

Hu Z, Zhang S, Zhang Y N, Wang D, Zeng H, and Liu L M (2015) Modulating the phase transition between metallic and semiconducting single-layer MoS2 and WS2 through size effects. *Phys. Chem. Chem. Phys.* **17**, 1099-1105.

Kan M, Wang J Y, Li X W, Zhang S H, Li Y W, Kawazoe Y, Sun Q, and Jena P (2014) Structures and phase transition of a MoS2 monolayer. *J. Phys. Chem. C* **118**, 1515-1522.

Kappera R, Voiry D, Yalcin S E, Branch B, Gupta G, Mohite A D, and Chhowalla M (2014) Phase-engineered low-resistance contacts for ultrathin MoS2 transistors. *Nat. Mater.* **13**, 1128-1134.

Lin Y C, Dumcenco D O, Huang Y S, and Suenaga K (2014) Atomic mechanism of the semiconducting-to-metallic phase transition in single-layered MoS2. *Nat. Nanotechnol.* **9**, 391-396.

Voiry D, Mohite A, and Chhowalla M (2015) Phase engineering of transition metal dichalcogenides. *Chem. Soc. Rev.* **44**, 2702-2712.

Zeng Z, Yin Z, Huang X, Li H, He Q, Lu G, Boey F, and Zhang H (2011) Single-layer semiconducting nanosheets: high-yield preparation and device fabrication. *Angew. Chem. Int. Ed. Engl.* **50**, 11093-11097.

Zhu J, Wang Z, Yu H, Li N, Zhang J, Meng J, Liao M, Zhao J, Lu X, Du L, Yang R, Shi D, Jiang Y, and Zhang G (2017) Argon plasma induced phase transition in monolayer MoS2. *J. Am. Chem. Soc.* **139**, 10216-10219.